https://doi.org/10.5194/egusphere-2025-4999
Preprint. Discussion started: 26 January 2026

Comparing the MEMS v1 model performance with MCMC and 4DEnVar calibration methods over a continental soil inventory

Toni Viskari[1], Tristan Quaife[2], Fernando Fahl[1], Yao Zhang[3], and Emanuele Lugato[1]

[1] European Commission, Joint Research Centre (JRC), Ispra, Italy

[2] National Centre for Earth Observation, Department of Meteorology, University of Reading, United Kingdom

[3] Natural Resource Ecology Lab, Colorado State University, USA

Correspondence to: Toni Viskari (toni.viskari@ec.europa.eu)

Abstract. An abundant amount of different data is required to calibrate soil organic carbon (SOC) models to represent ecosystems at large-scale. However, due to challenges related to model state projections, this calibration becomes very computationally heavy with traditional calibration methods. In this work, we test 4-Dimensional Ensemble Variational data assimilation (4DEnVar) method to parameterize the MEMS v1 SOC model using data from the LUCAS soil sampling network and compare its performance against MCMC calibration. Comparing the total SOC projections from both parameterizations and validation datasets showed similar improvements even though the produced parameter sets differed. A thorough analysis revealed that the detailed SOC states were not similar to a meaningful degree, but we also lacked information to determine which parameter set was closer to the truth. Our results here establish 4DEnVar as an applicable calibration method for SOC models but also highlight the need for more nuanced validation methods, as well careful examination how different data sets affect the model calibration.

1 Introduction

Soil organic carbon (SOC) stocks are a major component of the global carbon cycle (Scharlemann et al., 2014) and are inherently linked to surface vegetation, as the long-term SOC compounds forming them are produced by decomposition of plant litter (Cornwell *et al.*, 2008). Due to the importance of those stocks, they are a central part of national carbon budgets (van den Berg et al., 2020) and targeted by climate related policy (e.g. LULUCF, CRCF; Schlamadinger et a., 2007) aiming at enhancing carbon accumulation into the soils and improve terrestrial carbon sinks (Rumpel et al., 2020). All of this has also highlighted the need to improve the current soil related Monitoring, Reporting and Verification (MRV) systems (Bellassen *et al.*, 2015).

Soil inventory and numerous measurement campaigns, both temporary and continuous, have been set up to actively observe the soil carbon states within given regions and/or ecosystems (Smith et al., 2020). While these provide valuable information about the SOC stocks in that time window, also utilizing faster sample collections and analysis (Loria *et al*., 2024), they generally provide only information on the total SOC stocks. Indeed, current understanding of SOC cycling has been recently advanced separating the bulk soil into SOC fractions (Lavallee et al., 2019; Yu et al., 2022), notably the mineral-associated (MAOM) and the particulate organic matter carbon (POM). Though there are different methods to measure these short- and long-lived SOC fractions (Delahaie et al., 2024), they require considerable resources to be applicable on a large spatial scale. Thus, models are a crucial tool in both providing more cost-effective estimates of SOC states across landscapes, as well as their responses to both climate and environmental changes.

To this purpose, numerous models have been developed from simple first-order dynamic models such as RothC (Coleman and Jenkins, 1996) to more complicated non-linear models such as MIMICS (Wieder et al., 2014) and Millennial (Abramoff et al., 2022). However, the lack of detailed information both regarding the SOC state and drivers, such as litter and soil moisture, does affect the ability to reliably constrain the various processes included into the models. Therefore, it is necessary to calibrate the model with more measurements from different pedo-climatic and land cover conditions, in order to capture how they affect the SOC state. This, though, increases the computational cost of the calibration.

https://doi.org/10.5194/egusphere-2025-4999
Preprint. Discussion started: 26 January 2026

Additionally complicating matters is that even when using spatially diverse data for calibration, there are numerous assumptions regarding how that driver data is applied within the model that will affect not just model forward projections, but also the calibration process itself. For example, NPP is commonly used as a proxy for litterfall in SOC models (e.g. Abramoff et al., 2022; Pierson et al., 2022), with empirical work showing that the approach is justified (Matthews, 1997). How this NPP should be divided between above- and belowground biomass and, consequently between different model pools, depends on the ecosystem (Jevon et al., 2022; Cao et al., 2024) and is critical for determining the soil litter input. Without much more detailed information than is often available, these NPP/litter related parameter cannot be simultaneously calibrated with the SOC model parameters because of how fundamentally those values are connected; increasing/decreasing the amount of soil litter will simply result in an increase/decrease in decomposition rates to fit the measured SOC values. This is just one example of driver associated assumptions and a quick nimble calibration method is needed to assess how these uncertainties impact the calibration results.

The traditional grand standard for model calibration is the Monte Carlo Markov Chain Metropolis Hastings algorithm (MCMC; Geyer, 1992). This is a very computationally heavy approach with multiple variants having been developed over the years to make it more efficient in exploring the parameter space and avoid local likelihood maximas in its search for the most likely parameter sets (e.g Papaioannou et al., 2015; Vrugt, 2016). Due to the challenges discussed before, only computationally light SOC models can be calibrated within a practical time frame using large scale data (for example Tuomi et al., 2009). There have been workarounds presented, making assumptions about the initial state (Nemo, 2017; Mathers et al., 2023), using simpler calibration methods (Gurung et al, 2020) or taking advantage of machine learning approaches (Heuvelink et al., 2021). However, there remains a need for a fast and trustworthy calibration method for SOC models that would allow for easy experimentation on how different datasets affect the calibration or constraining new model dynamics being included.

Similarly to MCMC, in the Four-dimensional Variational data assimilation (4DVar; Le Dimet and Talagrand, 1986), a model projection is compared with observations and the new initial state for the next iteration is generated from this information. A key difference between MCMC and 4DVar is that the latter uses gradient descent methods to determine the next state instead of randomly sampling. While this method has initially been used more commonly for state data assimilation, for example, in weather forecast (Huang et al., 2009), it has also been successfully applied to calibrate ecosystem models (e.g. Raoult et al., 2016; Peylin et al., 2016; Pinnington et al. 2016). However, to implement 4Dvar with observations from multiple different times, an adjoint version of the model is needed which imposes its own challenges and limitations on the application (Thepaut and Courtier, 1991). Four-dimensional ensemble variational data assimilation (4DEnVar; Liu et al., 2008) is a novel data assimilation approach, where an ensemble is used to sidestep the need for the model adjoint. It has already been used for parameter calibration (Douglas et al., 2025; Pinnington et al. 2020) and is much faster than the traditional MCMC methods as it requires far fewer model iterations.

In the work presented here, we calibrated the MEMS v1 SOC model (Robertson et al., 2019) with both MCMC and 4DEnVar parameterization methods. Soil data from the Land Use/Land Cover Area Frame Survey (LUCAS) measurement network (Orgiazzi et al., 2018) were used for calibration and validation against estimated model parameters, assessing their performances relative to each other and the default parameters. Our hypothesis is that the 4DEnVar improves the model fit to the same degree as the MCMC, with much less computational cost.

Specifically, there are two objectives for the work presented here: the first is to test if 4DEnVar calibration performs as well as the MCMC calibration and examine if there are any meaningful differences in the resulting parameter sets; the second is to conduct a simple experiment where we made a change on how the NPP litter input was calculated. The intent here is to see both how this will affect the calibration and if the two methods respond similarly to the change.

2. Methods and data

2.1 LUCAS measurements

https://doi.org/10.5194/egusphere-2025-4999
Preprint. Discussion started: 26 January 2026

For the MEMS model calibration, we used the LUCAS points from a field campaign conducted in 2009 as reported in (Cotrufo et al., 2019; Lugato et al., 2021). This dataset comprises; 1) the main physico-chemical characteristic of topsoil (0-20 cm), including total SOC content for about 20.000 samples distributed across different land covers in the EU and UK; 2) a size-fraction of the bulk SOC into mineral-associated (MAOM) and particulate organic matter carbon (POM) in a representative sub-set of 350 samples. Both the calibration and total dataset are similarly distributed across ecosystems with approximately 73 % being grass- or croplands with the rest being various forest types. Figure 1 shows the LUCAS data points across Europe and the calculated SOC stock at each measurement site.

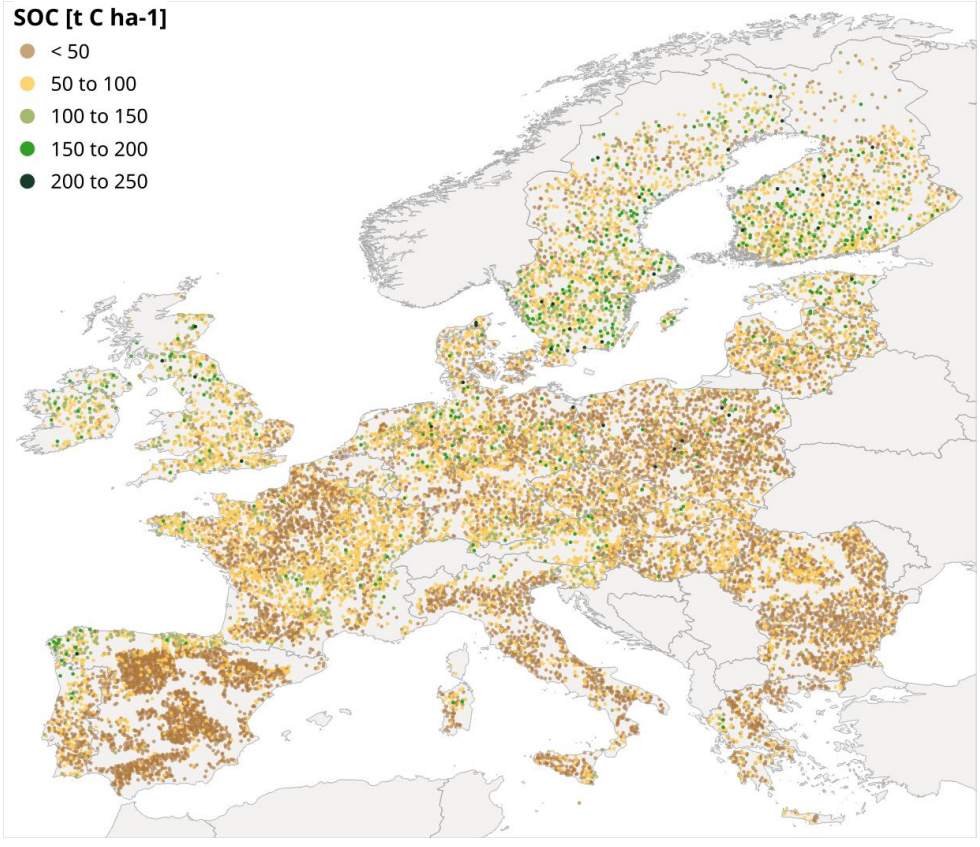

Figure 1: The LUCAS 2009 sampling point across Europe and their SOC stock.

For the calibration, the 348 LUCAS measurements from the 2009 campaign containing POM/MAOM fractions are used. The remaining 19 476 total SOC measurements were set aside for validation. In both allocations, measurements which were not classified as agricultural, grassland or forest were removed as well as all the sampling points where the driver data was not available. As a result, 322 datapoints are used for calibration and 17 430 for validation.

2.2 MEMS/Parameters chosen for calibration

The Microbial Efficiency-Matrix Stabilization (MEMS; Robertson et al., 2019) model is a novel soil organic carbon (SOC) model framework, which is built around the scientific understanding that the soil microbial pool modulates the SOC stocks. In the model, both surface vegetation and SOC decomposition are represented by multiple pools defined by their physical properties. There are several paths for carbon fluxes to transfer from one pool to another or lost as CO2, with the rate of change calculated on a daily timestep.

https://doi.org/10.5194/egusphere-2025-4999
Preprint. Discussion started: 26 January 2026

Since the calibration, here, focuses on the SOC stock, only the model equations affecting MEMS pools C5 (Heavy particulate organic matter), C8 (Dissolved organic matter), C9 (Mineral associated organic matter (MAOM)) and C10 (Light particulate organic matter) were considered in this work. While the surface vegetation decomposition pools do determine the litter input entering to soil C pools, those mechanics were not included in the calibration as the type of data required to constrain them was not available. Therefore, we used the default parameters values established in Robertson et al. (2019) for the surface processes.

The equations that govern the change in the relevant pools in MEMS are:

$$\frac{dC_5}{dt} = C_{5,in}^2 + C_{5,in}^3 + C_{5,in}^4 - T_{mod}k_5C_5 \quad (1)$$

$$\frac{dC_8}{dt} = C_{8,in}^5 + C_{8,in}^6 + C_{8,in}^{10} - sorp - DOC_{lch}C_8 - T_{mod}k_8C_8 \quad (2)$$

$$\frac{dC_9}{dt} = sorp - T_{mod}k_9C_9 \quad (3)$$

$$\frac{dC_{10}}{dt} = C_{10,in}^2 + C_{10,in}^3 - T_{mod}k_{10}C_{10} \quad (4)$$

Where C_i is the amount of carbon stored in pool i, $C_{i,in}^j$ is the carbon input to pool i from pool j as a result of the decomposition process and k_i is the decomposition rate for pool i. The leaching coefficient DOC_{lch} represents the dissolution of SOC to deeper soil layers and the temperature coefficient T_{mod} reflects how soil temperature affects the decomposition rate. In this work, T_{mod} is the same for all pools and follows the STANDCARB 2.0 model (Harmon et al., 2009).

The sorption coefficient *sorp* controls the flow of carbon between the microbial pool and the mineral associated carbon pool as determined by the equation

$$sorp = C_8 \frac{\frac{K_{lm}Q_{max}C_8}{1+K_{lm}C_8} - C_9}{Q_{max}} \quad (5)$$

$$Q_{max} = d \cdot \rho_{soil} \cdot (1 - p_{rock}) \cdot sc_{Conc} \quad (6)$$

$$sc_{conc} = sc_{slope} \cdot (1 - p_{sand}) + sc_{int} \quad (7)$$

In which K_{lm} is the langmuir isotherm term that depends on the soil pH, Q_{max} is the maximum absorption capacity of the soil, ρ_{soil} is the soil bulk density, p_{rock} is the rock percentage of the soil and p_{sand} is the sand percentage of the soil. The maximum concentration of fine fraction, sc_{conc}, is governed by the two coefficients sc_{int} and sc_{slope}. Consequently, those two parameters effectively control the saturation ratio for the MAOM pool.

The decomposition rate parameters k_5, k_8, k_9 and k_{10} were the central parameters chosen for calibration as well as sc_{int} and sc_{slope}. As the primary focus of this work is to compare the calibration methods, these parameters were simply chosen as a straight-forward test case. The boundary values are presented in Table 1. As prior values for our calibration, we also set randomly drawn and rounded values for the parameters near the middle of the set of the boundary conditions after testing that the model runs remained stable with these parameter values.

Name	Symbol	Prior	Minimum value	Maximum value
Decomposition rate for Pool C5	k_5	0.0008	0.0001	0.002
Decomposition rate for pool C8	k_8	0.001	0.0001	0.01
Decomposition rate for pool C9	k_9	0.000025	0.00001	0.00004
Decomposition rate for pool C10	k_{10}	0.0005	0.0001	0.0004
Saturation intercept	SC_{Icept}	10.0	5	20
Saturation slope	SC_{Slope}	0.25	0.1	0.4

Table 1: The calibrated parameters chosen for calibration, their baseline values as well as boundaries.

https://doi.org/10.5194/egusphere-2025-4999
Preprint. Discussion started: 26 January 2026

To determine how we divide the litter input to MEMS model pools, the site ecosystem type was assigned by the Corine Land Cover (Buttner, 2014). Following that, NPP is split into the MEMS model pools according to the following framework established in Robertson et al. (2019):

$$C_{1,input}(t) = (1 - f_{doc}^{eco}) f_{sol}^{eco} r^{eco} NPP(t) \quad (8)$$

$$C_{2,input}(t) = \left(1 - f_{sol}^{eco} - f_{lig}^{eco}\right) r^{eco} NPP(t) \quad (9)$$

$$C_{3,input}(t) = f_{lig}^{eco} r^{eco} NPP(t) \quad (10)$$

$$C_{6,input}(t) = f_{sol}^{eco} f_{doc}^{eco} r^{eco} NPP(t) \quad (11)$$

Where $C_{i,input}(t)$ is the carbon input to pool *i* from *NPP* at a given time *t* and *eco* refers to the ecosystem for the LUCAS point. Then, f_{sol} is the hot water extractable fraction of the litter input, f_{doc} is the cold-water extractable fraction of the water extractable fraction and f_{lig} is the acid-insoluble fraction of the of the litter input. It is important to note that these fractions are not the totality of the litter input and, while equations from 17 to 20 do sum up to the total NPP, the fractions presented here do not sum up to 1.

The coefficient values based on Campbell et al. (2016) are presented in Table 2. It is important to make two notes regarding these values. First, we are using a single fraction here and do not account for the uncertainty range provided in the work referenced. Second, only f_{sol} and f_{lig} fraction ranges are presented in Campbell et al., (2016). For f_{doc} we used a constant value across land covers in line with the work Robertson et al. (2019).

	NPP fraction	f_{sol}	f_{lig}	f_{doc}
Woody grassland	0.67	0.35	0.15	0.15
Pure grass	0.51	0.35	0.15	0.15
Sporadic grassland	0.59	0.35	0.15	0.15
Cropland	0.43	0.35	0.15	0.15
Mixture	0.77	0.375	0.295	0.15
Broadleaf	0.68	0.4	0.27	0.15
Conifer	0.78	0.35	0.32	0.15

Table 2: The fraction of NPP that is used for litter input and how it is divided into different litter compounds

2.3 MCMC

Markov Chain Monte Carlo (MCMC; Geyer, 1992) is a widely used Bayesian model parameterization method. The basis of this approach is straightforward: First values for the parameters chosen for calibration are drawn by randomly perturbing accepted parameter values and the model is run for given locations with these parameters. Assuming that the uncertainties are normally distributed, the total likelihood *F* of these projections, given observations that correspond to model predictions, is calculated with

$$F = \prod_{l=1}^{N_{obs}} (2\pi\sigma_l^2)^{\frac{1}{2}} e^{-\frac{1}{2}\sum_{l=1}^{N_{obs}} \frac{(x_l - y_l)^2}{\sigma_l}} \cdot \prod_{k=1}^{N_{par}} \left(2\pi\sigma_{\theta,k}^2\right)^{\frac{1}{2}} e^{-\frac{1}{2}\sum_{l=1}^{N_{par}} \frac{\left(\theta_k - \theta_{k,prior}\right)^2}{\sigma_{\theta,k}}} \quad (12)$$

Where *l* is the observation index, N_{obs} is the number of observations, σ is the associated uncertainty, x_l is the model projection with parameter set θ and y_l is the observation for index *l*. Furthermore, *k* is the parameter index, N_{par} is the number of parameters being estimated and Θ_{prior} is the prior estimate of parameters.

Once the likelihood is determined, it is compared to the likelihood of the previously accepted parameter set. If the new likelihood is higher, then that parameter set is automatically accepted and used as the parameters for the next iteration. However, if the new likelihood is lower than the previous one, there is still a probability that the

https://doi.org/10.5194/egusphere-2025-4999
Preprint. Discussion started: 26 January 2026

new parameter set will still be accepted depending on how close the new likelihood is to the previous accepted likelihood.

By allowing the lower likelihoods to be possibly accepted, MCMC also provides an acceptable parameter range, which can be used to represent the parameter uncertainties. This iterative process is repeated until a given convergence goal is satisfied (Roy, 2020).

For the study here, we used the MCMC framework established in Viskari et al. (2022), which utilizes the BayesianTools R-library (Hartig et al., 2019). The chosen MCMC algorithm is the Differential evolution Markov Chain with snooker updater (DEzs; ter Braak and Vrugt, 2008), where multiple calibration chains progress concurrently from different starting point with information shared between the chains at given intervals. This should lead to a more efficient and faster convergence of the calibration, especially as this approach makes it possible to parallelize the different chains.

Six chains were used for the calibration with the initial values for each chain randomly drawn from the prior parameter range. The MCMC was run for 100 000 accepted iterations with the convergence test and statistical values calculated from the last 10 000 iterations.

2.4 4-Dimensional Ensemble Variational assimilation

The foundational theory for 4-Dimensional Ensemble Variational data assimilation (4DEnVar) method is explained in Liu *et al.* (2008). The formulation established in Pinnington et al. (2020) was used as the basis for this work. In this section, we will provide a simplified description of the method as it applies to our purposes.

In traditional baseline 4-Dimensional Variational data assimilation (4DVar; Le Dimet and Talagrand, 1986), similarly to MCMC, the most likely state, i.e. the model parameter set, is solved by determining the minimum of the cost function J

$$J = \frac{1}{2}\left(\left(\boldsymbol{\theta} - \boldsymbol{\theta}_{prior}\right)^{T}\mathbf{B}^{-1}\left(\boldsymbol{\theta} - \boldsymbol{\theta}_{prior}\right) + \sum_{t=1}^{K}\left(M_{0\to t}(\boldsymbol{\theta}, \mathbf{x_0}) - \mathbf{y}_k\right)^{T}\mathbf{R}_t^{-1}\left(M_{0\to t}(\boldsymbol{\theta}, \mathbf{x_0}) - \mathbf{y}_k\right)\right) \quad (13)$$

In which $\boldsymbol{\theta}$ and $\boldsymbol{\theta}_{prior}$ are, respectively, the suggested and prior parameter value vectors, $\mathbf{B}$ is the prior parameter error covariance matrix and $\mathbf{R_t}$ is the observation error covariance matrix at the measurement time t. The model operator $M_{0\to t}$ calculates from the given parameters and the initial state $\mathbf{x_0}$ the output comparable to the observation vector $\mathbf{y_k}$. The measurement times in the chosen time window is represented by K.

Two brief notes on this formulation. First, it is essentially the same as exponent component in Eq 8, except that is written it in vector form. Second, in an effort to simplify the equations, we did not include anobservation operator component in the equations. All our observations are point measurements that can be directly compared with the model output, hence a separate observation operator was unnecessary for our purposes.

4DVar, like MCMC, is also an iterative approach that calculates the cost function with different state vectors to test if the cost function value decreases. However, with 4DVar, the iterations suggested after the first attempt are not randomly drawn, but rather determined by the gradient function

$$\nabla J = \mathbf{B}^{-1}\left(\boldsymbol{\theta} - \boldsymbol{\theta}_{prior}\right) + \sum_{t=1}^{K}\mathbf{M}_{0\to t}^{T}\mathbf{R}_t^{-1}\left(M_{0\to t}(\boldsymbol{\theta}, \mathbf{x_0}) - \mathbf{y}_k\right) \quad \mathbf{(14)}$$

Where $\mathbf{M}_{0\to t}^{\mathbf{T}}$ is the adjoint of the tangent-linear version $\mathbf{M}_{0\to t}$ of the model operator M.

The benefit of the gradient use is that it results in a value of zero for the state vector that produces the cost function minimum. Thus, gradient descent techniques (Ruder, 2016) are able to use the information from the gradient to efficiently locate the cost function minimum and the optimal state vector.

Naturally, there are challenges in applying this method. The core hurdle is the adjoint operator in equation Eq. 10, which is the transpose of the tangent-linear version of process model. Creating these model versions, though, is not a simple task and imposes a linearity assumption on the driving processes. Furthermore, since background error covariance matrix $\mathbf{B}$ can have non-diagonal terms representing error covariances, the inverse matrix can become computationally implausible to be calculated for larger systems.

https://doi.org/10.5194/egusphere-2025-4999
Preprint. Discussion started: 26 January 2026

In 4DEnVar, these issues are approached by expanding on the square root transform framework established in Tippett et al, 2003. Let us have an ensemble of model runs where, in our case, every ensemble has a different parameter set randomly drawn from the same baseline prior distribution. In the 4DEnVar formulation, this prior distribution is assumed normally distributed. For each ensemble member, we can then determine how its output differs from the prior parameter set output. These perturbations from the mean across the ensemble can be written in matrix format $\mathbf{\Theta'_b}$ as follows

$$\mathbf{\Theta'_b} = \frac{(\boldsymbol{\theta}^{b,1}-\bar{\boldsymbol{\theta}}^{b},\boldsymbol{\theta}^{b,2}-\bar{\boldsymbol{\theta}}^{b},\boldsymbol{\theta}^{b,3}-\bar{\boldsymbol{\theta}}^{b},\ldots,\boldsymbol{\theta}^{b,L}-\bar{\boldsymbol{\theta}}^{b})}{\sqrt{L-1}} \quad (15)$$

Where L is the ensemble size, $\boldsymbol{\theta}^{b,i}$ is the ith vector of the perturbation matrix, and $\bar{\boldsymbol{\theta}}^{b}$ is the average over the perturbations. In our case, the average over the perturbations is the same as the prior parameter vector $\boldsymbol{\theta}_{prior}$.

Since this matrix essentially represents the uncertainty related to the parameter values, the prior error covariance matrix $\mathbf{B}$ can be approximated as

$$\mathbf{B} \approx \mathbf{\Theta'_b}\mathbf{\Theta'^{T}_b} \quad (16)$$

We admit that in this formulation we ignore model structural error and assume the dominant error is from the parameter uncertainty.

Furthermore, we can define a vector w with the length of L that satisfies the equation

$$\mathbf{w} = \mathbf{\Theta'^{-1}_b}\left(\boldsymbol{\theta} - \boldsymbol{\theta}_{\mathbf{prior}}\right) \quad (17)$$

With these formulations and assumptions, the cost and gradient functions can be written as

$$\mathbf{J}(\mathbf{w}) = \frac{1}{2}\mathbf{w}.\mathbf{w}^{T} + \frac{1}{2}\sum_{t=1}^{K}(\mathbf{M}_{0\to t}\mathbf{\Theta'_b}\mathbf{w} + M_{0\to t}(\boldsymbol{\theta},\mathbf{x_0}) - \mathbf{y_k})^{\boldsymbol{T}}\mathbf{R_t^{-1}}(\mathbf{M}_{0\to t}\mathbf{\Theta'_b}\mathbf{w} + M_{0\to t}(\boldsymbol{\theta},\mathbf{x_0}) - \mathbf{y_k}) \quad (18)$$

$$\nabla J(\mathbf{w}) = \mathbf{w} + \sum_{t=1}^{K}\mathbf{\Theta'^{T}_b}\mathbf{M^{T}_{0\to t}}\mathbf{R_t^{-1}}(\mathbf{M}_{0\to t}\mathbf{\Theta'_b}\mathbf{w} + M_{0\to t}(\boldsymbol{\theta},\mathbf{x_0}) - \mathbf{y_k}) \quad (19)$$

With this new formulation, we can further approximate

$$\nabla J(\mathrm{w}) = \mathbf{w} + \sum_{t=1}^{K}(\mathbf{M_{0\to t}}\mathbf{\Theta'_b})^{\mathbf{T}}\mathbf{R_t^{-1}}(\mathbf{M}_{0\to t}\mathbf{\Theta'_b}\mathbf{w} + M_{0\to t}(\boldsymbol{\theta},\mathbf{x_0}) - \mathbf{y_k}) \quad (20)$$

This formulation removes the need for the adjoint version of the model. An additional benefit of the 4DEnVar method is that the gradient function value can be calculated for each ensemble member, since we are already running an ensemble to approximate the prior error covariance matrix. This information, then, makes straightforward determining the state estimate.

Compared to filter-based data assimilation methods (for example the Ensemble Kalman Filter; Evensen, 2003), the variational methods do not estimate the posterior uncertainty directly. However, we used the method established in Pinnington et al. (2021) to calculate the posterior distributions.

For the study here, we used the 4DEnVar algorithm provided in Quaife (2023). The gradient approach method used there is BFGS2 (Saito and Nakano, 1997) from the GNU Scientific Library (GSL).

The 4DEnVar methodology holds crucial benefits for our model calibration even beyond the reduction in computational cost compared to MCMC. Even though all the measurements used for calibration in this work are from the same year, the model outputs are steady state products that take hundreds of simulated years to produce. Hence, a 3-dimensional variational data assimilation (3DVar; Lorenc et al., 2000) cannot be applied and the adjoint of the model would be required, as the gradient function needs to be calculated at the start of the simulation. To complicate things further, the validity of the tangent-linear assumption would be questionable due to the length of the simulation in this situation.

2.5 Calibration setup and uncertainty attribution

After having set up the algorithmic framework for both calibration methods for the selected LUCAS data points, the first task was to complete a twin experiment, where we generated synthetic observations from with the model using a parameter set perturbed from the baseline parameters. Then, we performed the calibration with

https://doi.org/10.5194/egusphere-2025-4999
Preprint. Discussion started: 26 January 2026

these synthetic observations with their associated uncertainties set to be 1 % of those synthetic observations. This allows us to check if both methods were able to find the correct parameter sets in a situation where the true answer was known. For the 4dEnVar, the additional importance of these tests is to assess the ensemble size dimension required to consistently estimate the correct parameter set.

After the twin experiments have been conducted, the calibration itself is performed with the calibration dataset, before the validation runs are done for the validation dataset locations. In both situations the SOC is assumed to reflect a steady state. These runs were completed separately with two different f_{doc} values as a simple test regarding how NPP assumptions impact the MEMS model calibration.

For our test case study on the impact of the NPP assumptions on the parameterization, we repeated the calibrations with a small adjustment. We changed the f_{doc} value of grass- and croplands from 0.15 to 0.35. This increases the amount of the litter that is directly deposited to the soi and consequently adsorbed by the mineral matrixl instead of being lost during the transition between the surface and soil carbon pools. The logic behind this is that, in our expert opinion, it is likely that there will be the proportion of exudates and root litter inputted to the topsoil in grasslands and herbaceous crops to the litter pools compared to forests.. When calculating the steady state, the MEMS model is simulated over the period of 700 years from an initial state vector of (0.35, 0.35, 0.15, 0., 0., 0.15, 0., 0., 3000., 0., 0.) for the MEMS C1 to C9 pools, respectively. The values in pools C1, C2, C3 as well as C6 are used to ensure that there are no numerical errors at the start of the simulation and do no impact the steady state at all. For the MAOM pool C9, though, we initialised the model with some carbon already accumulated in order to reduce the number of simulated years required for steady state. Here, during calibration each LUCAS point is simulated for 700 years with the last output values compared to the measurements. At some sites, the MEMS model did not reach full steady state during this time, but the difference was within fractions of a percentage of the final steady state. As the change was so marginal already at this point, the shorter time period was chosen for computational efficiency.

As driver data at the European level, the model uses daily air temperature extracted from the E-OBS grid (Cornes et al., 2018). For each day of the year, an average temperature is calculated from a time series that spans from 2009-2018, with the temperature cycle then repeated for each year when calculating the steady state. Furthermore, the clay, sand and rock content of the soil as well as the soil bulk density and pH from LUCAS are used to determine soil properties driving SOC processes.

For Net Primary Production (NPP), first the average annual NPP over the decade 2000-2010 is extracted from the MODIS (Running et al., 2004) grid cell overlaying each LUCAS point. Then, a standard sine function is used to distribute the NPP across the year in order to produce the daily litter input. This approach was used instead of an averaged MODIS NPP annual time series as the NPP reflects the time when the atmospheric carbon is allocated into vegetation, not when the vegetation becomes litter input. Hence, we simplified the time series here, although it is not expected to meaningfully affect the modelling results.

The total SOC measurement uncertainties from the LUCAS dataset are used as the uncertainties in this application. Since LUCAS protocol requires to take a composite soil sample (out of 5 samples), the uncertainty was estimated propagating the error associated to all variables for calculating SOC stock (i.e. SOC content, depth, rock fragment). We run a Monte Carlo simulation with 5000 draws, using a standard deviation derived from the coefficient of variation reported in Goidts et al., 2009 for the microsite scale, with a similar sampling scheme of LUCAS. It is important to note, though, that these values are calculated from mixed samples. Thus, it may be an underestimation of the real uncertainty for several reasons as, for example, how LUCAS samples are overall representative of the field conditions. However, we do not have more information concerning the SOC measurement uncertainties available.

Regarding the MAOM fraction, there is no established uncertainty estimate to utilize. Because of that, we assigned an uncertainty where the standard deviation was 5 percent of the measured MAOM value. This choice was driven by both a discussion with the data collection team about the reliability of the data and to ensure an appropriate weight during the calibration process. When the initial cost function is calculated using the baseline MEMS parameter set with this uncertainty, the total SOC values account for approximately two thirds of the cost function value, with the MAOM fraction being responsible for the remainder.

The prior uncertainty assigned to the parameters introduced challenges in this work. With MCMC, because we only use the prior parameter value range for the initial sampling, we were able to apply a uniform uncertainty

https://doi.org/10.5194/egusphere-2025-4999
Preprint. Discussion started: 26 January 2026

distribution that was used to approximate the baseline parameter set in Robertson et al., 2019. For those parameters where the uncertainty was not provided, we approximated a wide enough uniform distribution around the assigned parameter value. The 4DEnVar method, though, requires a Gaussian uncertainty distribution as explained in section 2.4. As there is no prior information available, we used the baseline parameter values as the expected values, with the uncertainty represented by a standard deviation of 10 % of the parameter value. This uncertainty range, deliberately imposing a larger uncertainty, resulted in 4DEnVar calibration producing negative parameter values, which are naturally unrealistic. We will discuss the reasons and implications of this behaviour later.

In some studies, for example, uncertainty has also been a parameter estimated with MCMC (Cailleret et al., 2020). Considering the meaningful unknowns regarding the uncertainty approximations, this would be a valid approach to be applied here. We did not estimate uncertainties for the initial MCMC/4DEnVar comparison, as varying the uncertainties might cause issues with the gradient approach methods and, consequently, would make it difficult to interpret the differences between the two. After the comparison, though, we did perform a MCMC calibration of MEMS, where we also estimated a scaling parameter for both total SOC and MAOM fraction uncertainties. However, these results are not shown here, as the calibration did not result in a successful convergence.

3 Results

The twin experiments (not shown) established that both methods were able to produce the true parameters when calibrating against synthetic observations. For 4DEnVar, the experiments established that an ensemble size of 250 members consistently produced the parameters used to generate the synthetic observations and, thus, we chose to this ensemble size for the 4DEnVar consequents.

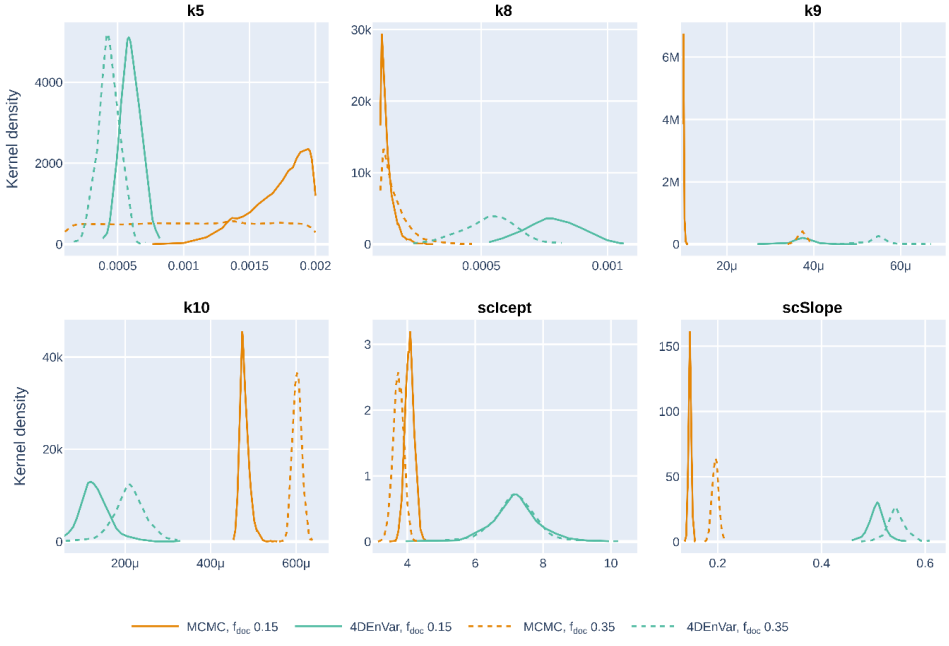

Figure 2: Estimated parameter distributions for both MCMC (orange) and 4DEnVar (green) calibrations with f_{doc} set to 0.15 (solid) and 0.35 (dashed). The μ indicates a multiplier of 10^{-6}.

The parameter distributions estimated by the MCMC and 4DEnVar calibration for both f_{doc} scenarios are presented in Figure 2. For clarity, the expected values from all the calibrations are in Table 3. From these, we

https://doi.org/10.5194/egusphere-2025-4999
Preprint. Discussion started: 26 January 2026

see that MCMC and 4DEnVar parameter sets differ meaningfully from each other in their value, but remain within the same range even when changing the NPP assumption. Furthermore, with the higher f_{doc} value, the uncertainty estimates with both methods end up being narrower, with the exception of k_5 for the MCMC calibration. It is also apparent that with three parameters (k_8, k_9 and Sc_{slope}), the MCMC produces expected values that are very close to the set boundaries when f_{doc} is set to 0.15 while, when set to 0.35, those distributions are clearly within the given parameter ranges. This indicates that with the lower f_{doc}, the MCMC calibration struggles to find an acceptable parameter set within the accepted range. Similarly, the uncertainties with the 4DEnVar are quite wide, which implies that it also cannot effectively locate an ideal parameter set.

The uncertainty distributions for 4DEnVar are generally wider than for MCMC in both cases. With 4DEnVar, we repeated the calibration multiple times to ascertain that the randomness associated with the ensemble selection did not result in meaningfully different parameter sets. While there was variance in the expected values, the standard deviation of the produced estimates was smaller than the standard uncertainty projection for any single estimation.

	4DEnVar	MCMC
k_5	0.0006/0.00043	0.0019/0.0019
k_8	0.00078/0.00053	0.0001/0.0001
k_9	0.000038/0.000055	0.00001/0.000037
k_{10}	0.00013/0.00021	0.00047/0.0006
SC_{Icept}	7.14/7.16	4.15/3.7
SC_{Slope}	0.51/0.54	0.144/0.197

Table 3: The expected parameter values produced by the different calibration methods and the baseline parameters. The first value is for f_{doc} 0.15, the second for f_{doc} 0.3s5.

To examine the impact of the new parameter sets, Figure 3 presents the differences between the measurements and model projections across all the validation sites. While the 4DEnVar parameter sets produces a somewhat symmetric error distribution around zero in both calibrations, with the lower f_{doc} there is a slight tendency towards negative errors. In contrast, the MCMC error distribution shows a notable lean towards positive errors for the lower f_{doc}, which largely disappears when the increasing direct litter input. Since the SOC errors here are calculated as the measurement minus the model projection, this means that positive errors reflect the parameter set systematically underestimating the SOC projections. It is notable that with the higher f_{doc}, the two error distributions are nearly identical.

https://doi.org/10.5194/egusphere-2025-4999
Preprint. Discussion started: 26 January 2026

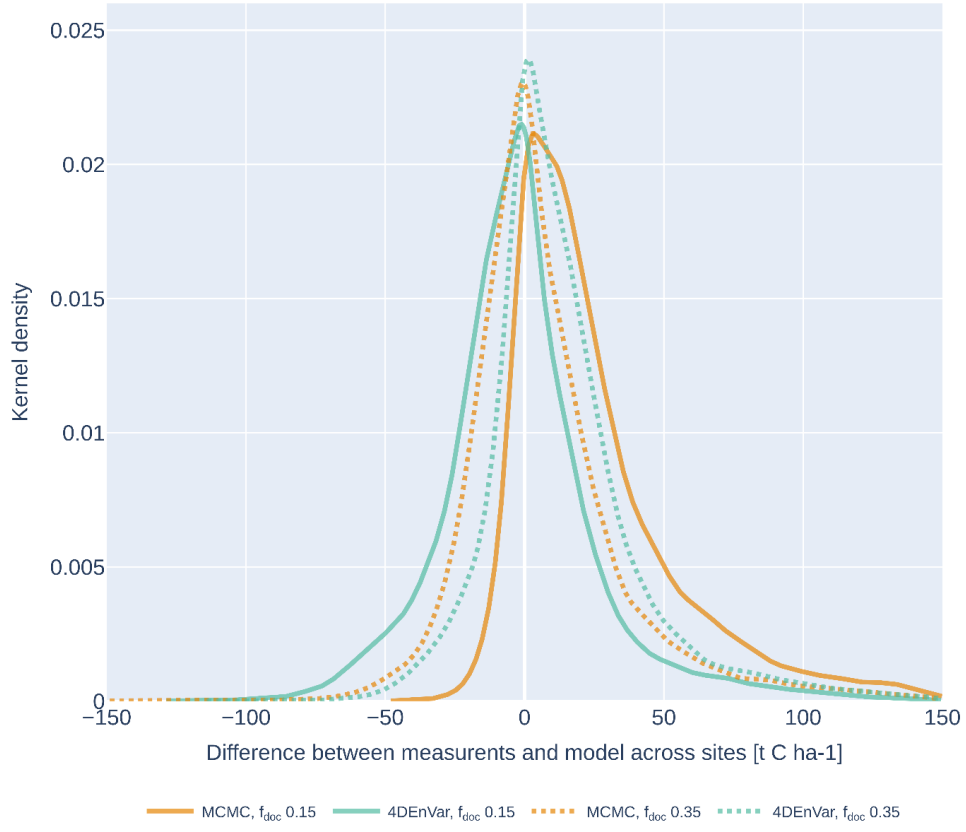

Figure 3: The validation dataset error distributions for both MCMC (orange) and 4DEnVar (green) calibrations with f_{doc} set to 0.15 (solid) and 0.35 (dashed).

To better comprehend what is causing these systematic errors when f_{doc}, is lower, we further examined the actual calibration fit with both approaches in this scenario. Figure 4a shows how well the model SOC projections follow the measurements and in Figure 4b the fit of the MAOM fraction with the 322 data points used for calibration. From these comparisons, it is evident that, while the 4DEnVar parameter set follows the measurement trend more closely than the MCMC, the latter calibration in turn replicates the MAOM:SOC fraction much better. We also note that there are also clear biases as the 4DEnVar parameters constantly underestimate the MAOM:SOC fraction, while there is a similar systemic underestimation of the total SOC with the MCMC parameters. When comparing the calibration fits for the higher f_{doc} (Not shown), the behaviour remains similar with calibration methods, although the differences between the measured and modelled values become smaller.

https://doi.org/10.5194/egusphere-2025-4999
Preprint. Discussion started: 26 January 2026

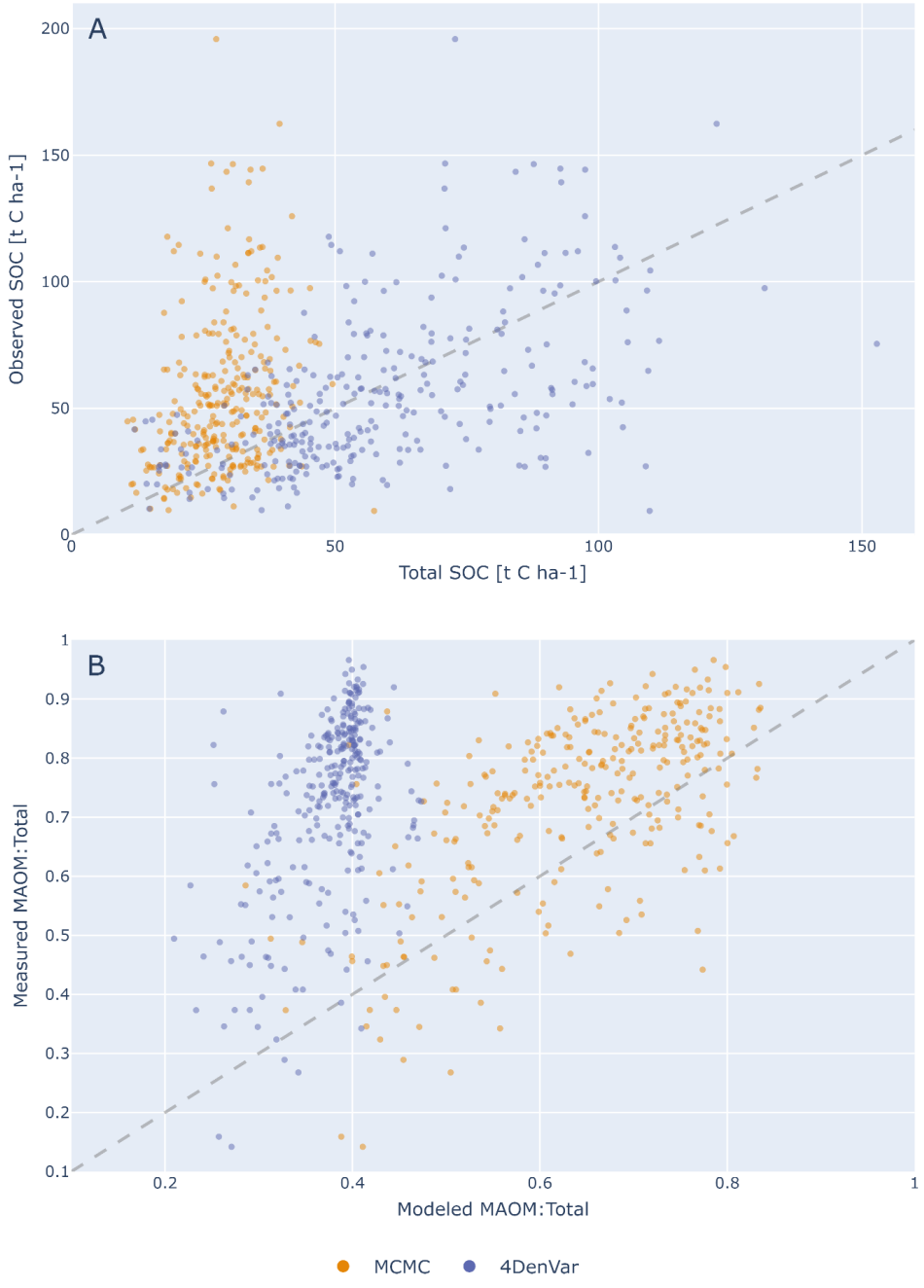

Figure 4: For the calibration dataset, comparison between the modelled and measured a) Total SOC value and b) MAOM:SOC fraction for both the MCMC and 4DEnVar calibrations

https://doi.org/10.5194/egusphere-2025-4999
Preprint. Discussion started: 26 January 2026

Figure 5 shows the spatial distribution of the errors in Europe for both the MCMC and 4DEnVar parameter sets. In the case of the lower f_{doc}, the MCMC underestimation is evident across Europe and, while the 4DEnVar map is more evenly distributed, there are also clearly more local overestimations than when f_{doc} is set higher. In the latter case, decrease in error can be seen across the whole Europe, with only a few clear areas, such as Nordic countries and the Iberian Peninsula, with consistent bias in the error. However, what is intriguing is that across central Europe, the prominent error points mirror each other. Where the MCMC parameter set produces overestimations, the 4DEnVar parameter set conversely results in underestimations.

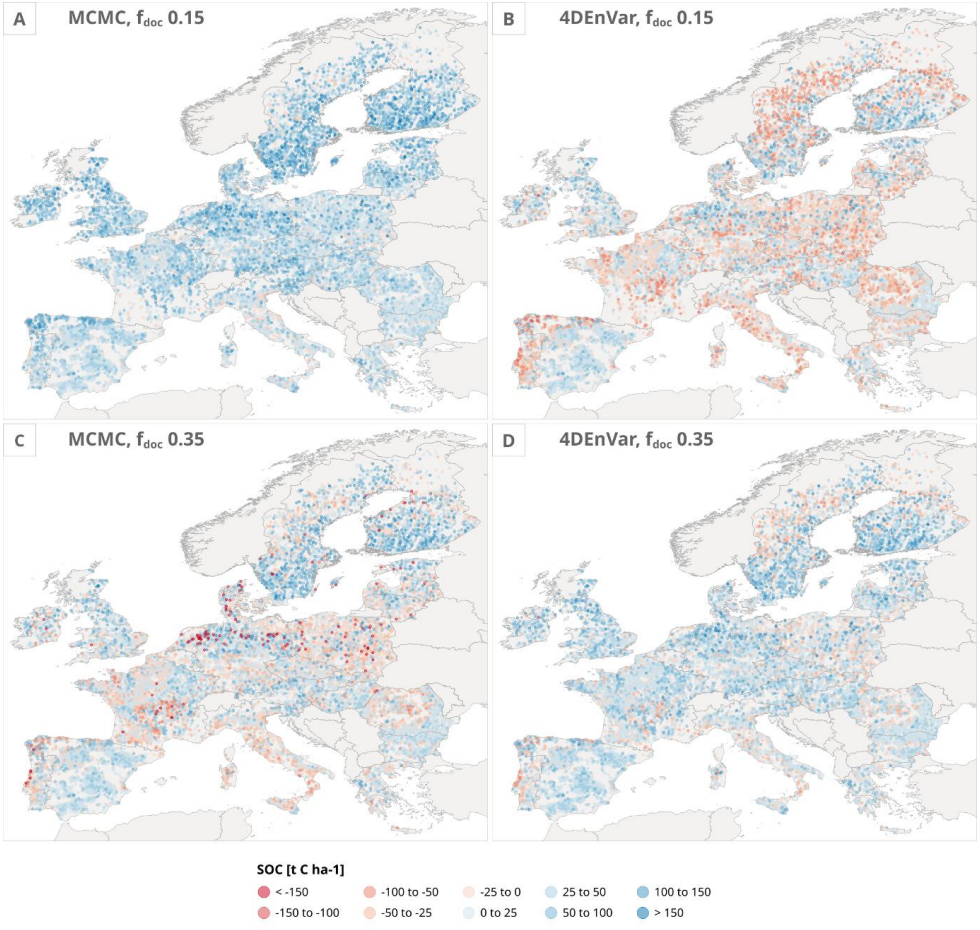

Figure 5: Spatial error distributions across the LUCAS validation sites for a) MCMC with f_{doc} value of 0.15, b) 4DEnVar with f_{doc} value of 0.15, c) MCMC with f_{doc} value of 0.35, and d) 4DEnVar with f_{doc} value of 0.35 parameter sets

Because of the pronounced errors when f_{doc} is set to the lower value, we further examined the relationship of the SOC error with the NPP used as an approximation of the total litter input (Figure 6). During this examination, it becomes evident that especially the MCMC parameter set projected a SOC underestimation clustered around low NPP values. When doing a further split into various ecosystems (Not shown), we see that the biases become much more pronounced with forest ecosystems.

https://doi.org/10.5194/egusphere-2025-4999
Preprint. Discussion started: 26 January 2026

409

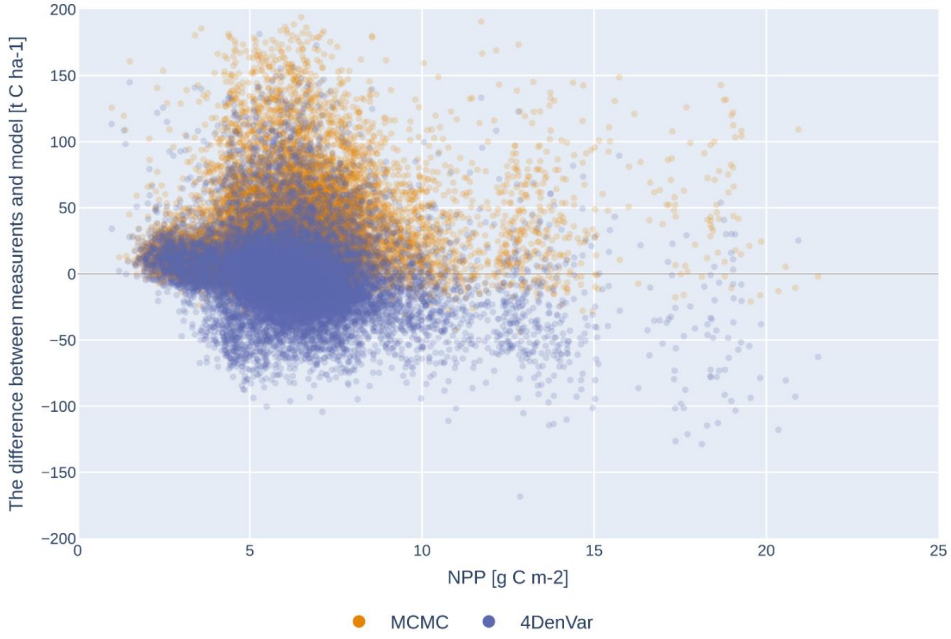

410

411 **Figure 6: Relationship between NPP and SOC projection error for both calibrated parameter sets**

412 Finally, we examined the POM, MAOM and MAOM:SOC fractions in relation to the total projected SOC stock
413 for the validation dataset with all calibrated parameter sets. Because of the systematic error when using the
414 lower f_{doc} and, due to the general behaviour remaining similar between the two scenarios, we are only
415 presenting the higher f_{doc} parameter set results here in Figure 7 for clarity. With the POM (Fig 7a) and MAOM
416 (Fig 7b), we can see a similar differences between the two calibrations resulting from the initial calibrations.
417 The MCMC parameterization still produces much higher MAOM stocks than 4DEnVar, and the latter
418 parameterization contrastingly results in higher POM stocks. Additionally, POM with MCMC parameters
419 remains at lower values than with the 4DEnVar parameters while, for the 4DEnVar parameters, MAOM hits a
420 ceiling sooner than for the MCMC parameters. To further examine the impact of these behaviours on the
421 projections, Figure 7c illustrated the relationship between the MAOM fraction and model error across all the
422 validation data points. Analysing the results further, we found that the very high SOC projections with both
423 MCMC and baseline parameters occurred in specific circumstances, where both NPP and annual temperatures
424 were low (not shown), and hence we attribute this to a structural issue within the model that arises in specific
425 conditions rather than the parameterization per se.

https://doi.org/10.5194/egusphere-2025-4999
Preprint. Discussion started: 26 January 2026

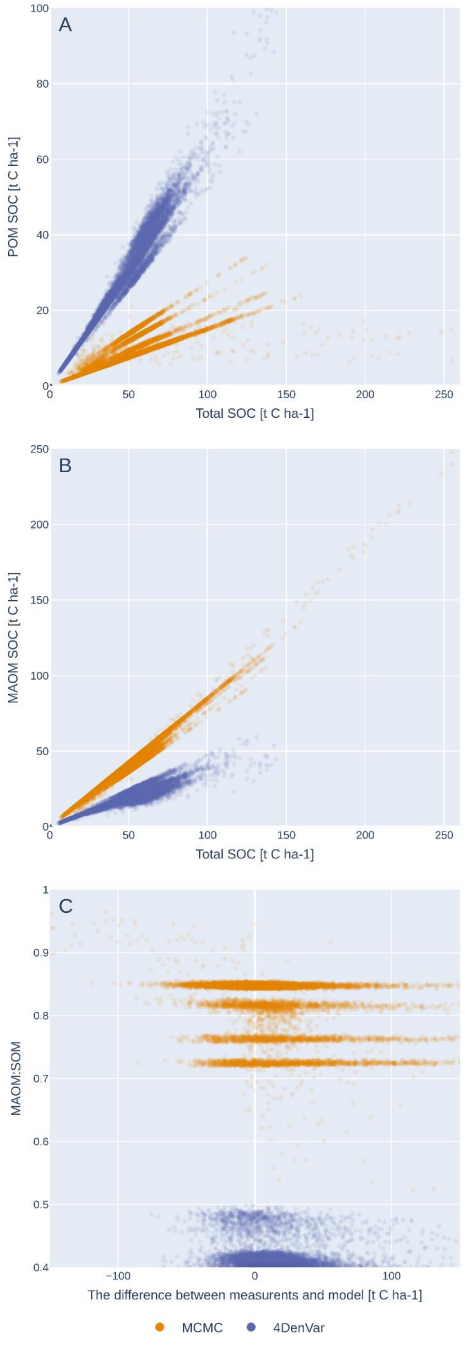

Figure 7: The model projected a) POM, b) MAOM stocks in relation to the total modelled SOC stocks as well as c) The MAOM:SOM ratio in relation to the model error across the LUCAS sites after f_{doc} was increased from 0.15 to 0.35.

https://doi.org/10.5194/egusphere-2025-4999
Preprint. Discussion started: 26 January 2026

4 Discussion

4.1 Comparison between the performances of MCMC and 4DEnVar calibration methods

As seen in the results, the 4DEnVar approach is a straightforward tool for calibrating the MEMS v1 model with LUCAS data, as valid as the MCMC approach. Both had issues with the first parameterization attempt when it came to the validation dataset, but performed similarly when the direct litter fraction to soil was increased. Hence, the central problem with the first calibration attempt was not due to the calibration method itself. This supports 4DEnVar as a meaningful approach for initial calibration of soil carbon models, especially considering the massive difference in the required computational costs. For MCMC, the 100 000 iterations used here took over a month to compute on our HPC server while, simulating the 250 ensemble members without using parallelization, took approximately four hours. It should be noted that the MCMC calibration did begin to converge to the final values already after 40 000 iterations, but there is a risk in accepting the first stable parameter set after such a relatively short calibration cycle. The computational cost for calibration from having to spin-up to steady state is a known issue with land system models in general (Raoult et al., 2025).

What is striking, though, is that the parameter sets produced by the two calibration methods in both litter distribution scenarios differ from each to a meaningful extent, even when they perform equally well with the validation dataset. In further analysis of the cost function (J) for each estimated parameter set, the MCMC calibration resulted in a meaningfully lower J with the initial f_{doc} while, with the increased f_{doc} (i.e. from 0.15 to 0.35), the difference in J between the two approached becomes marginal. However, when further looking at both total SOC and MAOM fractions measurements in both cases, the 4DEnVar produces a better match with total SOC while, conversely, the MCMC parameter set results in a closer fit with the MAOM fraction (MAOM: SOC) data. If we tighten the prior uncertainty used in the calibration, the 4DEnVar produces a different parameter set, though even those new parameters do still result in lower MAOM fractions in the validation dataset projections.

While we are not certain of what is driving these systematic differences between calibration sets, we hypothesize that one crucial component is that the total SOC and MAOM fraction measurements appear to incentivize contradicting model behaviours. This is especially evident when the f_{doc} is lower and there is less litter to distribute between the SOC pools. In that situation, MCMC is still able to find a solution by forcing a reduction in the decomposition rate for the MAOM pool and increasing the decomposition rate for the POM pool. This leads to a high MAOM fraction but at the cost of lower POM pool values and, consequently, a tendency to project lower SOC values. Meanwhile, this conflict between the two measurement types does seem to cause issues with the gradient approach method applied by 4DEnVar to determine the ideal parameter set. This could be because the disagreement between the data sources will create such a degree of noise in the likelihood space that determining a correct gradient descent from a collection of ensembles will become much more challenging. Simultaneously, though, this vulnerability in the 4DEnVar could be exploited in future work to quickly test if different measurement types and drivers are compatible within the model framework.

These results further highlight the fundamental impact of the priors on the calibration results, especially with the 4DEnVar approach, that has been recognized as a larger challenge in ecosystem modelling (Dietze, 2017). While experimenting with the initial setup, we found that the 4dEnVar calibration produced unrealistic parameter values with negative decomposition rates, if prior was set to be too loose. This remained true even when increasing the f_{doc} value, although then the uncertainty could be loosened slightly more. Our hypothesis is that, while the MCMC iterative approach allows setting boundaries for the region where the values are sampled, such hard constraints are not present with the 4DEnVar. Additionally, the 4DEnVar does rely on the first order Taylor expansion, making it vulnerable to non-linear behaviours. Thus, incongruities resulting from missing model processes such as soil moisture, for example, can drive the parameterization beyond acceptable values if there is not a sufficient prior constrain implemented. A further limitation is that the 4DEnVar algorithm used here draws the ensemble members by sampling the prior distribution. While this is a logical approach when those distributions are reliably approximated, here we do not know what the prior distributions are and must use a tight uncertainty range in order to avoid unrealistic estimations. Consequently, our application of 4DEnVar samples the parameter space in a more limited manner than would be preferable.

The lack of knowledge on prior distributions for the parameters is an obstacle that is further hindered by the lack of reliable measurement uncertainty estimates. An important aspect of Bayesian statistics is that the weight of an individual information source depends on how accurate it is in comparison to the other available information

https://doi.org/10.5194/egusphere-2025-4999
Preprint. Discussion started: 26 January 2026

sources. Hence, the width of the prior uncertainty that we can assign to constrain the parameter estimate to remain in a reasonable range is dependent on the measurement uncertainty. In this work, those uncertainties were so low that we had to use a relatively narrow prior parameter range for the 4DEnVar approach. Furthermore, as detailed in the Methods section, we do not have reliable approximations of the measured MAOC:SOC fraction uncertainties. Their uncertainty here is, thus, defined by how much weight we wished to give them in relation to the total SOC measurements. When we tested a larger measurement error, which in turn allowed us to increase the prior parameter distribution for the 4DEnVar without producing unrealistic estimates, the 4DEnVar ensembles also changed with the new values moving farther away from the baseline values. The implication is that the 4DEnVar is much more sensitive to the measurement uncertainty representation than MCMC, due to how the prior constraint is applied.

4.2 The impact of the NPP assumption on the calibrated parameter set performance

Our results clearly underline how the fundamental assumptions regarding the NPP, as a litter proxy, impact the model calibration results. The lower f_{doc} resulted in a noticeable bias on total SOC predictions, especially with regard to the MCMC calibration. Another encouraging aspect of the work is that the differences between the two calibration methods results remain consistent even when changing the litter input assumption. This supports the capability of using the quicker 4DEnVar calibration to explore the impact of the NPP assumptions on the parameterization as any signal noted there should be reflected also in MCMC results.

What complicates future work is that coefficients associated with litter input are challenging to calibrate simultaneously with parameters associated with SOC decomposition, as their influence on the SOC overlap too much. In addition, even attempting to calibrate the NPP/litter coefficients would first necessitate determining which exact coefficients would be calibrated. For example, in our case, there is first the question how well the MODIS NPP product represents reality for different systems. Then, part of that NPP is removed to represent economic activity before it is distributed to the four MEMS initial pools based on the three coefficients. Any of these three parts can be altered to change the final NPP input to the soil in different ways, but there is really no certainty at the moment what is the correct manner to better regulate the NPP based litter input. This complicated relationship in the surface vegetation driving litterfall and the SOC state has been shown in prior work such as in Raczka et al. (2021). There when they used remote sensing data to constrain their model state, while this improved their modelled aboveground biomass and carbon exchange accuracy, it also caused their modelled SOC accuracy to decrease because they were only using the aboveground data for both systems.

Naturally this is not to questioning the use of NPP as a litter input for soil carbon models. Rather it is another reminder on how important it is to be aware of the various assumptions related to the NPP and remain consistent with them while running the calibrated model in various systems. Additionally, when doing future SOC projections, the uncertainties related to the various NPP/litter assumptions should be considered during analysis.

The error distributions for both calibration methods when applying the higher litter input is in itself worthy of analysis. The MEMSv1 model used is lacking several dynamics that are known to impact soil carbon stock, such as soil moisture (Falloon et al., 2011), various nutrient cycles (Gardenas, et al., 2011; Feng et al., 2023) and mycorrhiza abundance (Hawkins et al., 2023). However, when considering the multitude of simplifications made to calculate the steady state approximations using parameters calibrated with data from 322 sites, the error distribution for the 17 000+ validation sites is remarkably narrow. Which raises question how much of a further performance issue could be expected with addition of new processes? And, consequently, how can this limited data be used to evaluate which processes are most important for future projections?

Notably, while the spatial presentation of the model error under the higher f_{doc} shows only few regions where the differences between the two model errors are consistently larger than 10 tons of carbon per hectare, such as the Nordic countries, the MAOM fraction projections by the two model calibrations differ systematically to a meaningful degree. For instance, 4DEnVar calibration resulted in a higher turnover rate of the MAOM pool, which in turn causes lower MAOM stocks. Both calibration methods are adjusting the parameters to produce lower total SOC, as the baseline parameters tend to overestimate the SOC stocks, but they solve the issue with very different representations of the internal SOC state that would have a major impact on future projections. With the current available information, it is not possible to evaluate which of the two states is more realistic; while the MCMC modelled MAOM fractions are on average high for all ecosystems (Georgiou et al., 2022), the LUCAS dataset leans towards arable soils where the MAOM fraction is expected to be larger in the top layer than for forests (Schrumpf et al, 2013; Sokol et al, 2022).

https://doi.org/10.5194/egusphere-2025-4999
Preprint. Discussion started: 26 January 2026

These outcomes emphasise the importance of carefully considering how model performance improvements are assessed with large-scale datasets such as the LUCAS measurement data, since the total SOC seems not sufficient. This is especially relevant as the model validation should be a crucial aspect of model choice regarding different SOC sequestration projects (Garsia et al., 2023). New measurement analysis methods allow for more efficient POM/MAOM fractioning of SOC samples (Delahaie et al., 2023), thus providing more detailed measurements to use during validation. However, as our results show, the SOC fractions might not be compatible with the total SOC measurements within the model context and indicate that there are missing processes within our model framework. Consequently, their value might be rather to evaluate what missing processes are needed within the model than validate existing parameterizations. Another approach for evaluation could be to examine the model performance within sub-regions or individual ecosystems instead of weighing it against the total dataset at once. A more nuanced approach to do this would be to use a hierarchical Bayesian approach (Gelman and Hill, 2007), but that requires more research on the applicability of that approach in solving the challenges highlighted by our results.

5 Conclusions

Calibrating soil organic carbon (SOC) models with large scale data sets is always a challenge due to the computational cost involved. Furthermore, numerous assumptions are made regarding model drivers that can potentially deeply affect the parameterization. In our work presented in this article, we have shown that 4DEnVar parameterization produces as good validation performance as the traditional and more cumbersome MCMC DEzs algorithm. However, the parameter sets produced by the calibration methods meaningfully differed from each other as did the model states they projected. Even though the total SOCs were similar, the difference between shorter lived POM and longer lived MAOM compounds was large enough to notably impact future projections. We also conducted a simple experiment to assess the impact of a slight change in how the soil litter input was calculated. From those results, we did see that this change did result in meaningfully different parameterizations, but also that the comparisons between the two methods remained similar. The work here highlights how further consideration is required how to evaluate the model performances, especially on a larger scale. However, they also establish the fast 4DEnVar as a valid exploration tool that allows testing various scenarios with much more ease than the traditional MCMC approach.

Data/Code availability

The MEMS v1 model version, the calibration algorithms as well as all the data used for calibration and validation is available on Zenodo at https://doi.org/10.5281/zenodo.17314989 (Viskari et al. (2025).

Author contributions

TV is the primary author of the manuscript and was responsible for creating the calibration framework as well as analysing the results. TQ provided expert assistance in implementing the 4DEnVar and insight into the results. FF helped setting up the environmental driver data and created the graphical presentation of the results. YZ is one of the creators the MEMS v1 model and offered expertise on prior calibration approaches with the model. EL is PI of the project that this research is a part of and was responsible for the LUCAS dataset model efforts.

Competing interests:

The authors declare that they have no conflict of interests.

Acknowledgments

https://doi.org/10.5194/egusphere-2025-4999
Preprint. Discussion started: 26 January 2026

580 This research was supported by the Carbon Removal on Land project, an administrative arrangement (n. 36662)
581 between the Directorate-General Climate (DG-CLIMA) and the Joint Research Centre of the European
582 Commission. Tristan Quaife was funded under the International Programme of the UKRI National Centre for
583 Earth Observation (NE/X006328/1).

https://doi.org/10.5194/egusphere-2025-4999
Preprint. Discussion started: 26 January 2026

References:

Abramoff, R.Z., Guenet, B., Zhang, H., Georgiou, K., Xu, X., Viscarra Rossel, R.A., Yuan, W., And Ciais, P.: Improved global-scale predictions of soil carbon stocks with Millenial Version 2. *Soil Biol Biochem*, **164**, 108466, 2022

Bellassen, V., Stephan, N., Afriat, M., Alberola, E., Barker, A., Chang, J.-P., Chiquet, C., Cochran, I., Deheza, M., Dimopoulos, C., Foucherot, C., Jacquier, G., Morel, R., Robinson, R., and Shishlov, I.: Monitoring, reporting and verifying emissions in the climate economy. *Nature Climate Change*, **5(4)**, 319-328, 2015

Buttner, G: "CORINE land cover and land cover change products." In *Land use and land cover mapping in Europe: practices & trends* (pp. 55-74). Dordrecht: Springer Netherlands

Cailleret, M., Bircher, N., Hartif, F., Hulsmann, L., and Bugmann, H.: Bayesian calibration of a growth-dependent tree mortality model to simulate the dynamics of European temperate forests. *Ecol Appl*, **30**, e02021, 10.1002/eap.2021, 2020

Campbell, E.E., Parton, W.J., Soong, J.L., Paustian, K., Hobbs, N.T., and Cotrufo, M.F.: Using litter chemistry controls on microbial processes on partition litter carbon fluxes with Litter Decomposition and Leaching (LIDEL) model. *Soil Biol Biochem*, **100**, 160-174, 2016

Cao, J., Li, Y., Biswas, A., Holden, N.M., Adamowski, J.F., Wang, F., Hong, S., and Qin, Y.: Grassland biomass allocation across continents and grazing practices and its response to climate and altitude. *Agric For Met*, 356, 110176, 10.1016/j.agrformet.2024.110176, 2024

Coleman, K., and Jenkinson, D. S.: RothC-26.3-A Model for the turnover of carbon in soil. In *Evaluation of soil organic matter models: Using existing long-term datasets* (pp. 237-246). Berlin, Heidelberg: Springer Berlin Heidelberg, 1996

Cornes, R.C., Van Der Schrier, G., Van Den Besselaar, E.J., and Jones, P.D.: An ensemble version of the E-OBS temperature and precipitation data sets. *J Geophys Res*, **123(17)**, 9391-9409, 2018

Cornwell, W. K., Cornelissen, J. H. C., Amatangelo, K., Dorrepaal, E., Eviner, V. T., Godoy, O., Hobbie, S. E., Hoorens, B., Kurokawa, H., Perez-Harguindeguy, N., Quested, H. M., Santiage, L. S., Wardle, D. A., Wright, I. J., Aerts, R., Allison, S. D., van Bodegom, P., Brovkin, V., Chatain, A., Callaghan, T. V., Diaz, S., Garnier, E., Gurvich, D. E., Kazakou, E., Klein, J. A., Read, J., Reich, P. B., Soudzilovskaia, N. A., Vaieretti, M. V., and Westoby, M.: Plant species traits are the predominant control on litter decomposition rates within biomes worldwide, *Ecol. Lett.*, **11**, 1065–1071, 2008.

Cotrufo, M.F., Ranalli, M.G., Haddix, M.L., Six, J., and Lugato, E.: Soil carbon storage informed by particulate and mineral-associated organic matter. *Nat Geosci*, **12**, 989-994, 2019

Delahaie, A.A., Barre, P., Baudin, F., Arrouays, D., Bispo, A., Boulonne, L., Chenu, C., Jolivet, C., Martin, M.P., Ratie, C., Saby, N.P.A., Savignac, F., and Cecillon, L.: Elemental stoichiometry and Rock-Eval® thermal stability of organic matter in French topsoils. Soil, 9, 209-229, 10.5194/soil-9-209-2023, 2023

Delahaie, A.A., Cecillon, L., Stojanova, M., Abiven, S., Arbelet, P., Arrouays, D., Baudin, F., Bispo, A., Boulonne, L., Chenu, C., Heinonsalo, J., Jolivet, C., Karhu, K., Martin, M., Pacini, L., Poeplau, C., Ratie, C., Roudier, P., Saby, N.P.A., Savignac, F., and Barre, P.: Investigating the complementarity of thermal and physical soil organic carbon fractions. *Soil*, **10(2)**, 795-812, 2024

Dietze, M.: Ecological forecasting. Princeton University Press. 10.1515/9781400885459, 2017

Douglas, N., Quaife, T., and Bannister, R.: Exploring a hybrid ensemble–variational data assimilation technique (4DEnVar) with a simple ecosystem carbon model. *Environmental Model Softw*, 106361, 2025

Evensen, G.: The ensemble Kalman filter: Theoretical formulation and practical implementation. *Ocean dyn*, **53**, 343-367, 2003

Falloon, P., Jones, C.D., Ades, M., and Paul, K.: Direct soil moisture controls of future global soil carbon changes: An important source of uncertainty. *Glob Biochem Cycles*, **25(3)**, 10.1029/2010GB003938, 2011

https://doi.org/10.5194/egusphere-2025-4999
Preprint. Discussion started: 26 January 2026

629 Feng, J., Song, Y., and Zhu, B.: Ecosystem-dependent responses of soil carbon storage to phosphorus
630 enrichment. *New Phytol*, **238(6)**, 2363-2374, 10.1111/nph.18907, 2023

631 Gardenas, A.I., Agren, G.I., Bird, J.A., Clarholm, M., Hallin, S., Ineson, P., Katterer, T., Knicker, H., Nilsson,
632 S.I., Nasholm, T., Ogle, S., Paustian, K., Persson, T., and Stendahl, J.: Knowledge gaps in soil carbon and
633 nitrogen interactions – From molecular to global scale. *Soil Biol Biochem*, **43(4)**, 702-717,
634 10.1016/j.soilbio.2010.04.006, 2011

635 Garsia, A., Moinet, A., Vazquez, C., Creamer, R.E., and Moinet, G.Y.K.: The challenge of selecting an
636 appropriate soil organic carbon simulation model: A comprehensive global review and validation assessment.
637 Glob Change Biol, 29(20), 5760-5774, 10.1111/gcb.16896, 2023

638 Gelman, A. and Hill, J.: Data analysis using regression and multilevel/hierarchical models. Cambridge
639 University Press, Cambridge, 2007

640 Georgiou, K., Jackson, R.B., Vinduskova, O., Abramoff, R.Z., Ahlstrom, A., Feng, W., Harden, J.W.,
641 Pellegrini, A.F.A., Polley, H.W., Soong, J.L., Riley, W.J., and Torn, M.S.: Global stocks and capacity of
642 mineral-associated soil organic carbon. *Nat Commun*, **13**, 3797, 2022

643 Geyer, C.J.: Practical Markov Chain Monte Carlo. *Stat Sci*, **7(4)**, 473-483, 1992

644 Goidts, E., van Wesemael, B., and Crucifix, M.: Magnitude and sources of uncertainties in soil organic carbon
645 (SOC) stock assessment at various scales. *Eur J Soil Sci*, **60**, 723-739, 10.1111/j.1365-2389.2009.01157.x, 2009

646 Gurung, R.B., Ogle, S.M., Breidt, F.J., Williams, S.A., and Parton, W.J.: Bayesian calibration of the DayCent
647 ecosystem model to simulate soil organic carbon dynamics and reduce model uncertainty. *Geoderma*, **376**,
648 114529, 10.1016/j.geoderma.2020.114529, 2020

649 Hartig, F., Minunno, F., Paul, S., Cameron, D., Ott, T., and Pichler, M.: BayesianTools: General-Purpose
650 MCMC and SMC Samples and Tools for Bayesian Statistics. R package version 0.1.8, https://CRAN.R-
651 project.org/package=BayesianTools (last access: 2 May 2025), 2019.

652 Harmon, M. E., Moreno, A., and Domingo, J. B.: Effects of partial harvest on the carbon stores in Douglas-
653 fir/western hemlock forests: a simulation study. *Ecosystems*, **12**, 777-791, 2009

654 Hawkins, H.-J., Cargill, R.I.M., Van Nuland, M.E., Hagen, S.C., Field, K.J., Sheldrake, M., Soudzilovskaia,
655 N.A., and Kiers, E.T.: Mycorrhizal mycelium as a global carbon pool. *Current Biology*, **33(11)**, R560-R573,
656 2023

657 Heuvelink, G.B.M., Angelini, M.E., Poggio, L., Bai, Z., Batjes, N.H., van den Bosch, R., Bossio, D., Estella, S.,
658 Lehmann, J., Olmedo, G.F., and Sanderman, J.: Machine learning in space and time for modelling soil organic
659 carbon change. *Eur J Soil Sci*, **72(4)**, 1607-1623, 2021

660 Huang, X.-Y., Xiao, Q., Barker, D.M., Zhang, X., Michalakes, J., Huang, W., Henderson, T., Bray, J., Chen, Y.,
661 Ma, Z., Dudhia, J., Guo, Y., Zhang, X., Won, D.-J., Lin, H.-C., and Kuo, Y.-H.: Four-dimensional Variational
662 Data Assimilation for WRF: Formulation and Preliminary Results. *Mon Weather Rev*, 137(1), 299-314,
663 10.1175/2008MWR2577.1, 2009

664 Jevon, F.V., Polussa, A., Lang, A.K., Munger, J.W., Wood, S.A., Wieder, W.R., and Bradford, M.A.: Patterns
665 and controls of aboveground litter inputs to temperate forests. *Biogeochemistry*, **161**, 335-352, 2022

666 Lavallee, J.M., Soong, J.L., and Cotrufo, M.F.: Conceptualizing soil organic matter into particulate and mineral-
667 associated forms to address global change in the 21st century. *Glob Change Biol*, **26(1)**, 261-273,
668 10.1111/gcb.14859, 2020

669 Le Dimet, F., and Talagrand, O.: Variational algorithms for analysis and assimilation of meteorological
670 observations: Theoretic aspects. *Tellus*, ***38A***, 97–110, 1986

671 Liu, C., Xiao, Q. and Wang, B.: An Ensemble-Based Four-Dimensional Variational Data Assimilation Scheme.
672 Part I: Technical Formulation and Preliminary Test. *Mon Weather Rev*, **136(9)**, 3363-3373,
673 10.1175/2008MWR2312.1, 2008

https://doi.org/10.5194/egusphere-2025-4999
Preprint. Discussion started: 26 January 2026

Lorenc, A.C., Ballard, S.P., Bell, R.S., Ingleby, N.B., Andrews, P.L.F., Barker, D.M., Bray, J.R., Clayton, A.M., Dalby, T., Li, D., Payne, T.J., and Saunders, F.W.: The Met Office global three-dimensional variational data assimilation scheme. *Quarterly J Royal Meteorol Soc*, **126(570)**, 2991-3012, 2000

Loria, N., Lai, R., and Chandra, R.: Handheld In Situ Methods for Soil Organic Carbon Assessment. *Sustainability*, **16(13)**, 5592, 2024

Lugato, E., Lavallee, J.M., Haddix, M.L., Panaganos, P., and Cotrufo, M.F.: Different climate sensitivity of particulate and mineral-associated soil organic matter. *Nature Geoscience*, **14(5)**, 295-300, 2021

Mathers, C., Black, C.K., Segal, B.D., Gurung, R.B, Zhang, Y., Easter, M.J., Williams, S., Motew, M., Campbell, E.E., Brummit, C.D., Paustian, K., and Kumar, A.A.: Validating DayCent-CR for cropland soil carbon offset reporting at a national scale. *Geoderma*, **438**, 116647, 10.1016/j.geoderma.2023.116647, 2023

Matthews, E.: Global litter production, pools, and turnover times: Estimates from measurement data and regression models. *J Geophys Res Atmos*, **102(D15)**, 18771-18800, 1997

Nemo, Klumpp, K., Coleman, K., Dondini, M., Goulding, K., Hasting, A., Jones, M.B., Leifeld, J., Osborne, B., Saunders, M., Scott, T., Teh, Y.A., and Smith, P.: Soil Organic Carbon (SOC) Equilibrium and Model Initialisation Methods: an Application to the Rothamsted Carbon (RothC) Model. *Environ Model Assess*, **22**, 215-229, 2017

Orgiazzi, A., Ballabio, C., Panagos, P., Jones, A., and Fernande-Ugalde, O.: LUCAS soil, the largest expandable soil dataset for Europe: a review. *Eur J Soil Sci*, **69**, 140-153, 2018

Papaioannou, I., Betz, W., Zwirglmaier, K., and Straub, D.: MCMC algorithms for subset simulation. *Probabilistic Eng Mech*, *41*, 89-103, 2015

Peylin, P., Bacour, C., MacBean, N., Leonard, S., Rayner, P., Kuppel, S., Koffi, E., Kane, A., Maignan, F., Chevallier, F., Ciais, P., and Prunet, P.: A new stepwise carbon cycle data assimilation system using multiple data streams to constrain the simulated land surface carbon cycle. *Geosci Model Dev*, **9**, 3321-3346, 10.5194/gmd-9-3321-2016, 2016

Pierson, D., Lohse, K.A., Wieder, W.R., Patton, N.R., Facer, J., de Graaff, M.-A., Georgiou, K., Seyfried, M.S., Flerchinger, G., and Will, R.: Optimizing process-based models to predict current and future soil organic carbon stocks at high-resolution. *Sci Rep*, **12**, 10824, 2022

Pinnington, E.M., Casella, E., Dance, S.L., Lawless, A.S., Morison, J.I., Nichols, N.K., Wilkinson, M. and Quaife, T.L.: Investigating the role of prior and observation error correlations in improving a model forecast of forest carbon balance using Four-dimensional Variational data assimilation. *Agric For Meteorol*, *228*, 299-314, 2016

Pinnington, E., Quaife, T., Lawless, A., Williams, K., Arkebauer, T., and Scoby, D.: The Land Variational Ensemble Data Assimilation Framework: LAVENDAR v1.0.0. *Geosci Model Dev*, 13, 55-69, 10.5194/gmd-13-55-2020, 2020

Pinnington, E., Amezcua, J., Cooper, E., Dadson, S., Ellis, R., Peng, J., Robinson, E., Morrison, R., Osborne, S., and Quaife, T.: Improving soil moisture prediction of a high-resolution land surface model by parameterising pedotransfer function through assimilation of SMAP satellite data. *Hydrol Earth Sys Sci*, **25(3)**, 1617-1641, 10.5194/hess-25-1617-2021, 2021

Quaife, T.: C implementation of 4DEnVar using the GSL. Github repository, https://github.com/tquaife/4DEnVar_engine, 2023

Raczka, B., Hoar, T.J., Duerte, H.F., Fox, A.M., Anderson, J.L., Bowling, D.R., and Lin, J.C.: Improving CLM5.0 Biomass and Carbon Exchange Across the Western United States Using a Data Assimilation System. J Adv Model Earth Sys, e2020MS002421, 10.1029/2020MS002421, 2021

Raoult, N.M., Jupp, T.E, Cox, P.M., and Luke, C.M.: Land-surface parameter optimisation using data assimilation techniques: the adJULES system v1.0. *Geosci Model Dev*, **9**, 2833-2852, 10.5194/gmd-9-2833-2016, 2016

https://doi.org/10.5194/egusphere-2025-4999
Preprint. Discussion started: 26 January 2026

Raoult, N., Douglas, N., MacBean, N., Kolassa, J., Quaife, T., Roberts, A.G., et al.: Parameter estimation in land surface models: Challenges and opportunities with data assimilation and machine learning. *J Adv Model Earth Sys*, **17**, e2024MS004733, 10.1029/2024MS004733, 2025

Robertson, A.D., Paustian, K., Ogle, S., Wallenstein, M.D., Lugato, E., and Cotrufo, M.F.: Unifying soil organic matter formation and persistence frameworks: the MEMS model. *Biogeosciences*, **16**, 1225-1248, 10.5194/bg-16-1225-2019, 2019

Roy, V.: Convergence diagnostics for markov chain monte carlo. *Annu Rev Stat Appl*, **7(1)**, 387-412, 2020

Ruder, S.: An overview of gradient descent optimization algorithms. *arXiv preprint arXiv:1609.04747*,2016

Rumpel, C., Amiraslani, F., Chenu, C., Cardenas, M.G., Kaonga, M., Koutika, L.-S., Ladha, J., Madari, B., Shirato, Y., Smith, P., Soudi, B., Soussana, J.-F., Whitehead, D., and Wollenberg, E.: The 4p1000 initiative: opportunities, limitations and challenges for implementing soil organic carbon sequestration as a sustainable development strategy. *Ambio*, **49(1)**, 350-360, 10.1007/s13280-019-01165-2, 2020

Running, S.W., Nemani, R.R., Heinsch, F.A., Zhao, M., Reeves, M., and Hashimoto, H.: A continuous satellite-derived measure of global terrestrial production. *BioScience*, **54**, 547-560, 2004

Saito, K., and Nakano, R.: Partial BFGS update and efficient step-length calculation for three-layer neural network. *Neural computation*, **9(1)**, 123-141, 1997

Scharlemann, J.P.W., Tanner, E.V.J., Hiederer, R., and Kapos, V.: Global soil carbon: understanding the largest terrestrial carbon pool. *Carbon Manag*, **5**, 81-91, doi.org/10.4155/cmt.13.77, 2014

Schlamadinger, B., Bird, N., Johns, T., Brown, S., Canadell, J., Ciccarese, L., Dutschke, M., Fiedler, J., Fischlin, A., Fearnside, P., Corner, F., Freibauer, A., Frumhoff, P., Hoehne, N., Kirschbaum, M.U.F., Labat, A., Marland, G., Michaelowa, A., Montanarella, L., Moutinho, P., Murdiyarso, D., Pena, N., Pingoud, K., Rakonczay, Z., Rametsteiner, E., Rock, J., Sanz, M.J., Schneider, U.A., Shvidenko, A., Skutsch, M., Smith, P., Somogyi, Z., Trines, E., Ward, M., and Yamagata, Y.: A synopsis of land use, land-use change and forestry (LULUCF) under the Kyoto Protocol and Marrakech Accords. *Environ Sci Policy*, **10(4)**, 271-282, 2007

Schrumpf, M., Kaiser, K., Guggenberger, G., Persson, T., Kogel-Knabner, I., and Schulze, E.-D.: Storage and stability of organic carbon in soils as related to depth, occlusion with aggregates, and attachment to minerals. *Biogeosciences*, **10**, 1675-1691, 10.5194/bg-10-1675-2013, 2013

Smith, P., Soussana, J.-F., Angers, D., Schipper, L., Chenu, C., Rasse, D.P., Batjes, N.H., van Egmond, F., McNeill, S., Kuhnert, M., Arias-Navarro, C., Olesen, J.E., Chirinda, N., Fornara, D., Wollenberg, E., Alvaro-Fuentes, J., Sanz-Cobena, A., and Klumpp, K.: How to measure, report and verify soil carbon change to realize the potential of soil carbon sequestration for atmospheric greenhouse gas removal. *Glob Change Biol*, **26(1)**, 219-241, 2020

Sokol, N.W., Whalen, E.D., Jilling, A., Kallenbach, C., Pett-Ridge, J., and Georgiou, K.: Global distribution, formation and fate of mineral-associated soil organic matter under changing climate: A trait-based perspective. *Funct Ecol*, **36(6)**, 1411-1429, 10.1111/1365-2435.14040, 2022

ter Braak, C.J.F., and Vrugt, J.A.: Differential evolution Markov chain with snooker updater and fewer chains. *Stat Comput*, **18**, 435e446, 10.1007/s11222-008-9104-9, 2008

Thepaut, J.N., and Courtier, P.: Four-dimensional variational data assimilation using the adjoint of a multilevel primitive-equation model. *Quarterly J Royal Meteorol Soc*, **117(502)**, 1225-1254, 1991

Tippett, M.K., Anderson, J.L., Bishop, C.K., Hamill, T.M.,

Tuomi, M., Thum, T., Jarvinen, H., Fronzek, S., Berg, B., Harmon, M., Trofymow, J.A., Sevanto, S., and Liski, J.: Leaf litter decomposition – Estimates of global variability based on the Yasso07 model. Ecol Modell, 220, 3362-3371, 10.1016/j.ecolmodel.2009.05.016, 2009

van den Berg, N.J., van Soest, H.L., Hof, A.F., den Elzen, M.G.J., van Vuuren, D.P., Chen, W., Drouet, L., Emmerling, J., Fujimori, S., Hoehne, N., Koberle, A.C., McCollum, D., Schaeffer, R., Shekhar, S.,

https://doi.org/10.5194/egusphere-2025-4999
Preprint. Discussion started: 26 January 2026

765 Vishwanathan, S.S., Vrontisi, Z., and Blok, K.: Implications of various effort-sharing approaches for national
766 carbon budgets and emission pathways. *Clim Change*, **162**, 1805-1822, 2020

767 Viskari, T., Pusa, J., Fer, I., Repo, A., Vira, J., and Liski, J.: Calibrating the soil organic carbon model Yasso20
768 with multiple datasets. *Geosci Model Dev*, *15*(4), 1735-1752, 10.5194/gmd-15-1735-2022, 2022

769 Viskari, T., Quaife, F., Fahl, F., Zhang, Y., and Lugato, E.: Comparing the MEMS v1 model performance with
770 MCMC and 4DEnVar calibration methods over a continental soil inventory,
771 https://doi.org/10.5281/zenodo.17314989, (Last accessed October 10 2025), 2025

772 Vrugt, J.A.: Markov chain Monte Carlo simulation using theDream software package: Theory, concepts, and
773 MATLAB implementation. Environ Model Softw, 75, 273-316, 10.1016/j.envsoft.2015.08.013, 2016

774 Wieder, W. R., Grandy, A. S., Kallenbach, C. M., and Bonan, G. B.: Integrating microbial physiology and
775 physio-chemical principles in soils with the MIcrobial-MIneral Carbon Stabilization (MIMICS)
776 model. *Biogeosciences*, *11*(14), 3899-3917, 2014

777 Yu, W., Huang, W., Weintraub-Leff, S.R., and Hall, S.J.: Where and why do particulate organic matter (POM)
778 and mineral-associated organic matter (MAOM) differ among diverse soils? *Soil Biol Biochem*, **172**, 108756,
779 2022